Electronic Supplementary Material (ESI) for Dalton Transactions.
This journal is © The Royal Society of Chemistry 2023

Supporting information

Copper(II) complex enhanced chemodynamic therapy through GSH depletion and autophagy flow blockade

Wen-Ying Shen[#a,b], Chun-Peng Jia[#a], Li-Yi Liao[a], Liu-Lin Chen[a], Cheng-Cheng Yuan[a], Yun-Qiong Gu[a], Yang-Han Liu[a], Hong Liang[*a], Zhen-Feng Chen[*a]

[a]State Key Laboratory for Chemistry and Molecular Engineering of Medicinal Resources, Collaborative Innovation Center for Guangxi Ethnic Medicine, School of Chemistry and Pharmaceutical Sciences, Guangxi Normal University, Guilin 541004, P. R. China. E-mail: chenzf@gxnu.edu.cn (Z.-F. Chen); hliang@gxnu.edu.cn (H. Liang)

[b]Scientific Research Center, Guilin Medical University, Guilin, 541199, P. R China

Table of Contents

Materials and experimental procedures

Materials

Bax [E63], Bcl-2 [E17], DDIT-3 [9C8] (CHOP) antibodies were purchased from Abcam (Cambridge, UK). Phospho-eIF2α (Ser51) (D9G8) antibody was purchased from Cell Signaling Technology (CA, USA). Phospho-PERK (Thr982) antibody was purchased from Invitrogen (CA, USA).

Experimental procedures

•OH determination by EPR

Equal molar copper(II) complex and GSH were dissolved in DMF and distilled water, respectively. And they were mixed and reacted for 5 min at r. t.. H_2O_2 and DMPO were added to the mixture. Subsequently, the mixture was diluted with distilled water, and H_2O_2 and DMPO were added to detect •OH by Bruker A300 Spectrometer.

Cytotoxic activity

The cells were incubated for 48 h after dosing. MTT was added for 4-6 h. The upper liquid was poured out, DMSO was added, shaken for 5 min, and the absorbance at 570 and 490 nm was read. The growth inhibition was calculated as: $(1\text{-}OD_{test}/OD_{control}) \times 100\%$.

Intracellular GSH/GSSG ratio detection

T24 cells were treated with **C2** (18 μM) for 48 h. Cells were collected and washed. The remaining steps of GSH and GSSG content detection were carried out according to the manufacturer's instructions. Both GSH and GSSG test kits were purchased from Solarbio (China). Finally, GSH/GSSG ratio was obtained by dividing GSH by GSSG.

Cellular Ca^{2+} detection

T24 cells were treated with **C2** (12, 15, 18 μM), respectively. After 24 hours, cells were stained with Ca^{2+} fluorescent dye Fura-3AM for 30 minutes. Subsequently, the treated cells were further washed with PBS, and the changes of cellular Ca^{2+} were immediately detected by flow cytometry.

Caspase-3/9 activity determination

T24 cells were treated with **C2** (12, 15, 18 μM), respectively. After 24 hours, cells were collected and stained with FITC-DEVD-FMK (caspase-3) and FITC-LEHD-FMK (caspase-9) at 37 ℃ for at least 30 minutes. And flow cytometry was used to analyze the cells with activated caspase.

Structural characterization of all compounds

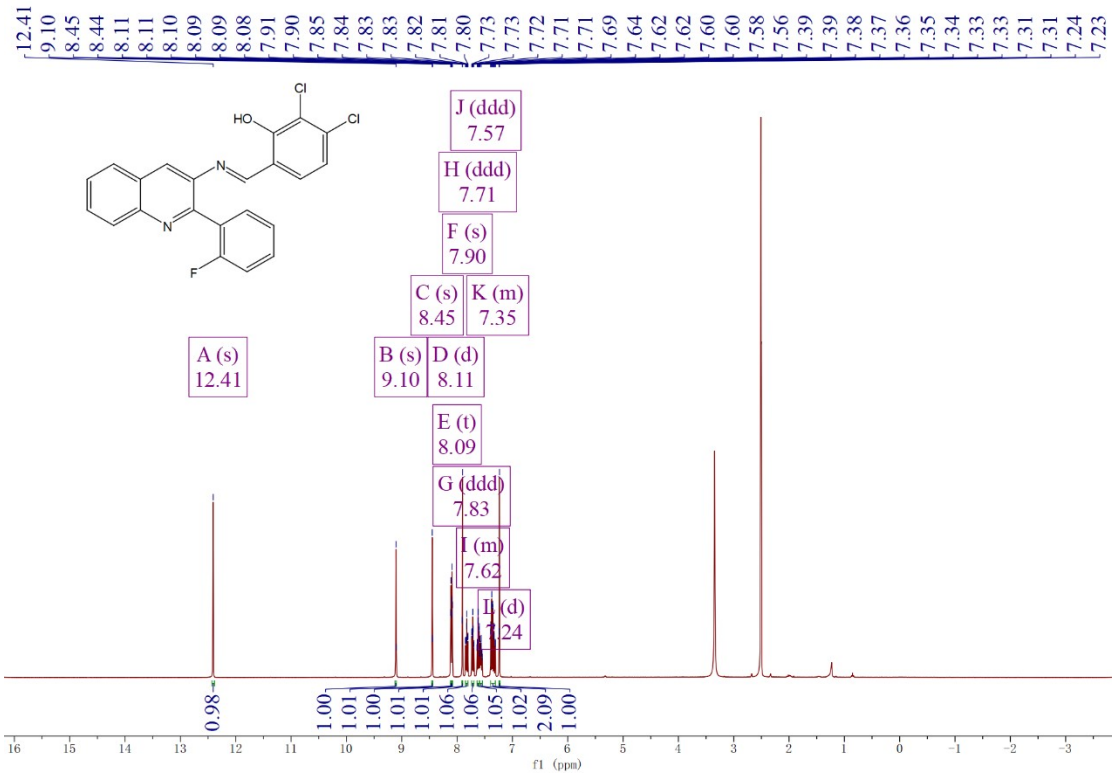

Figure S1. ^{1}H NMR (400MHZ, DMSO-d_6) spectrum of **L^1**

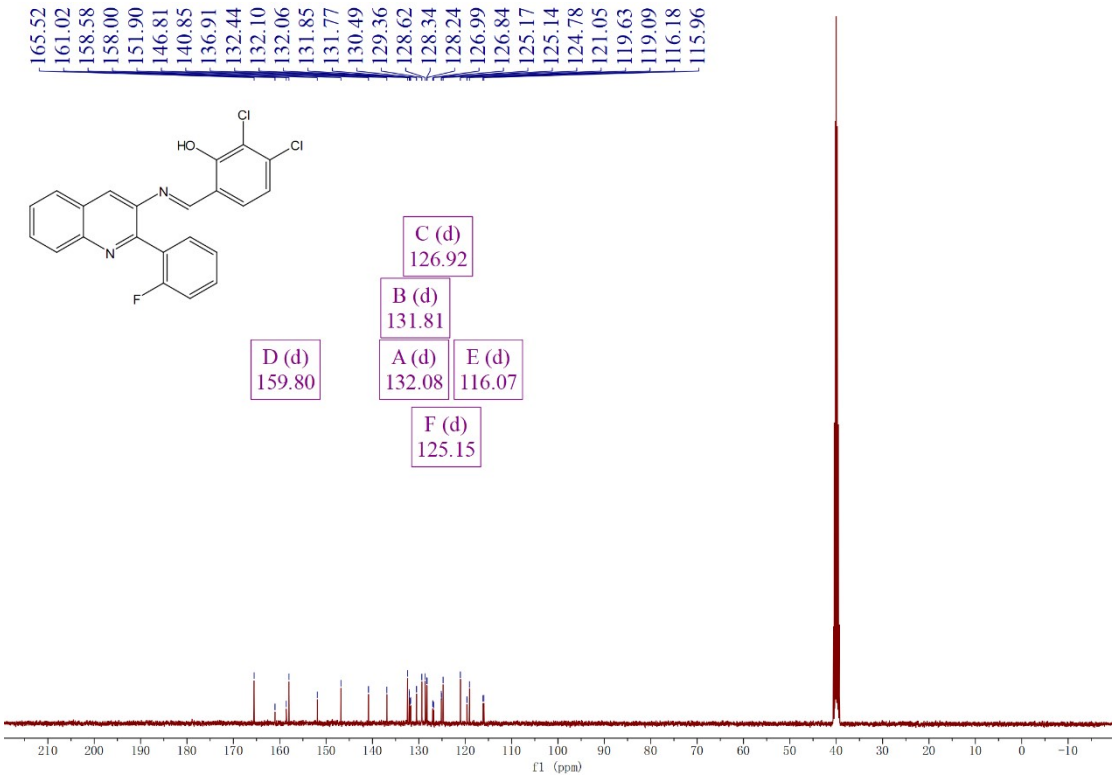

Figure S2. ^{13}C NMR (100MHZ, DMSO-d_6) spectrum of **L^1**

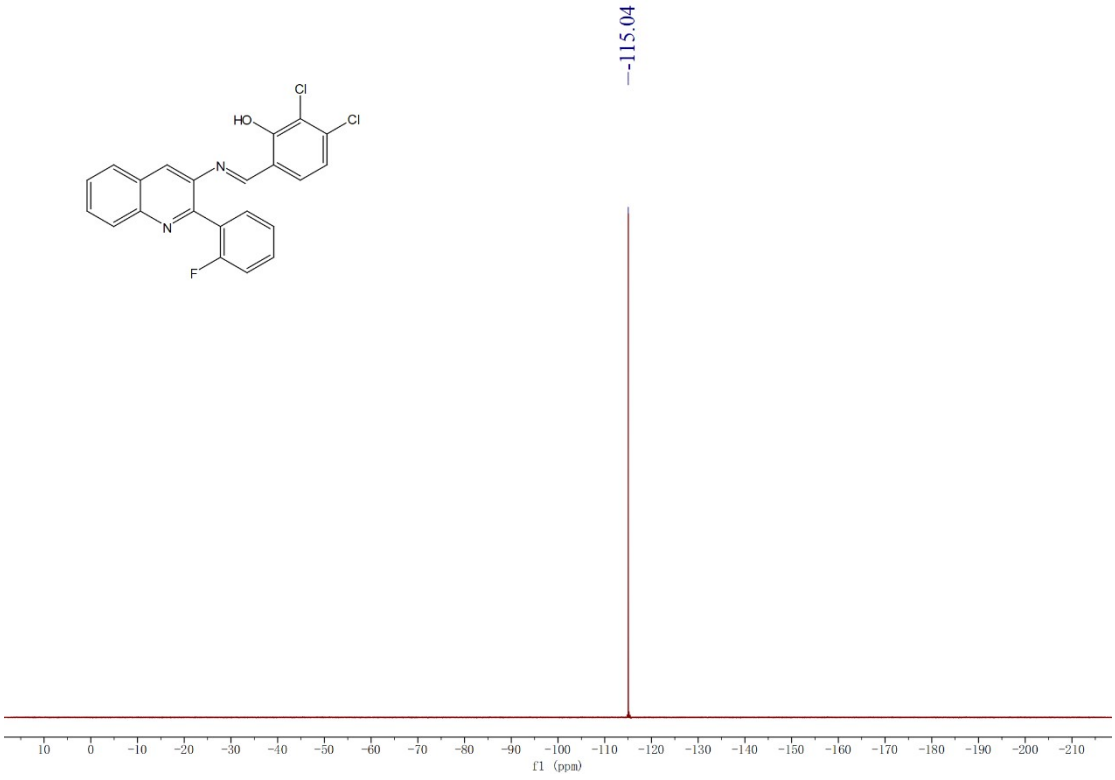

Figure S3. ^{19}F NMR (376MHZ, DMSO-d_6) spectrum of **L^1**

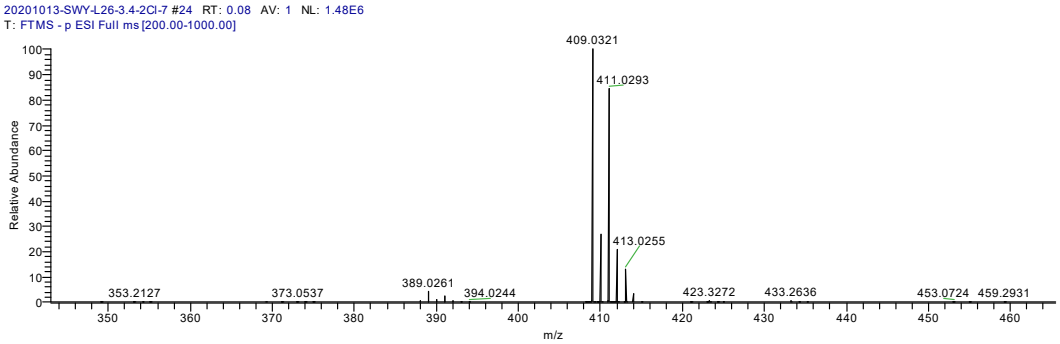

Figure S4. HRMS spectrum of **L**[1]

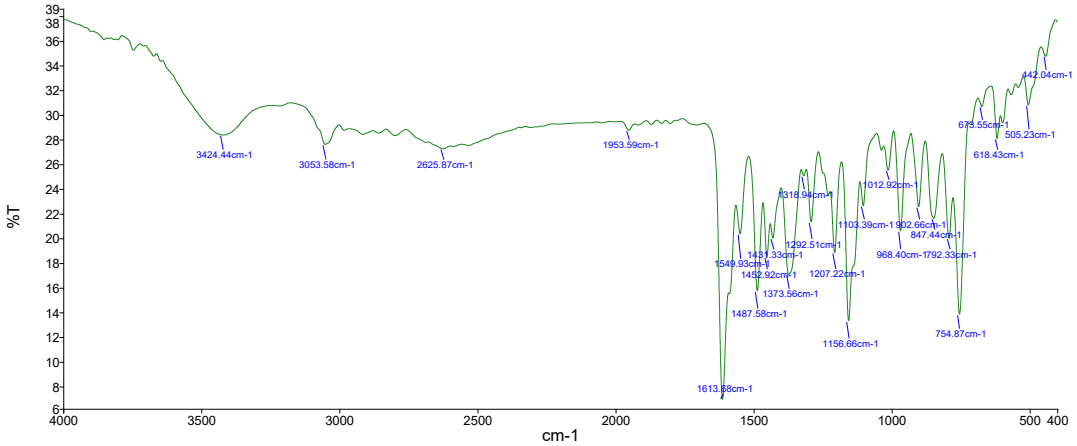

Figure S5. FT-IR spectrum of **L**[1]

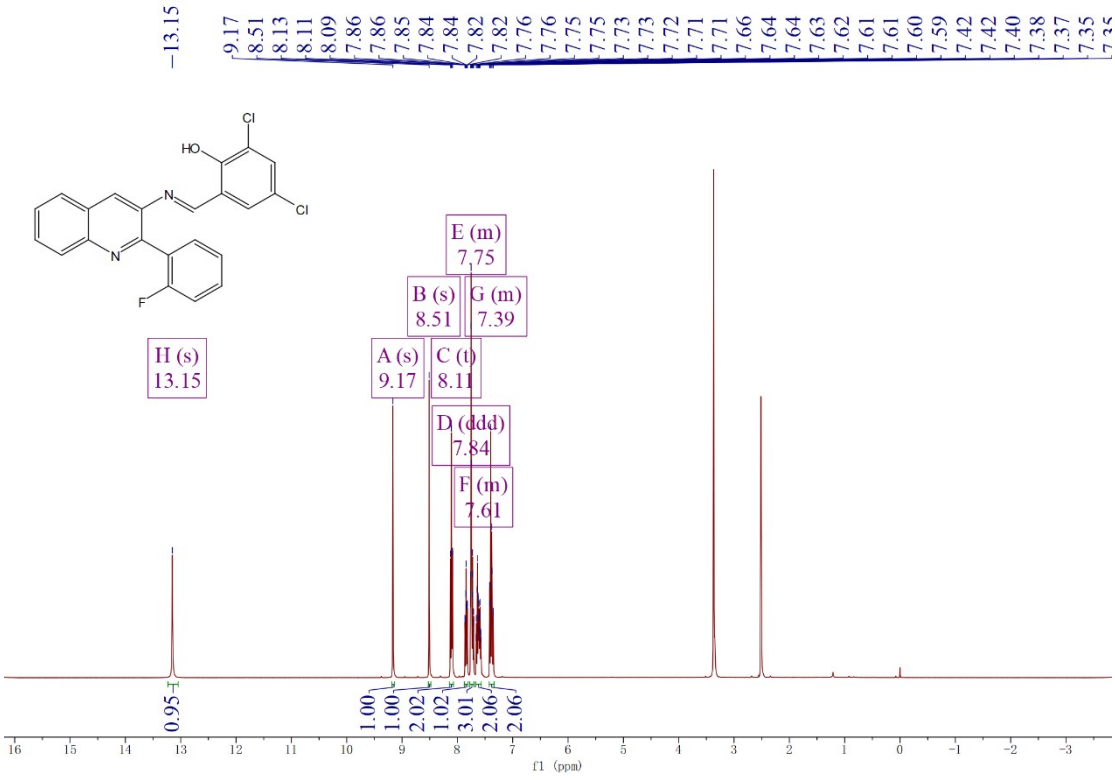

Figure S6.[1]H NMR (400MHZ, DMSO-d_6) spectrum of **L**[2]

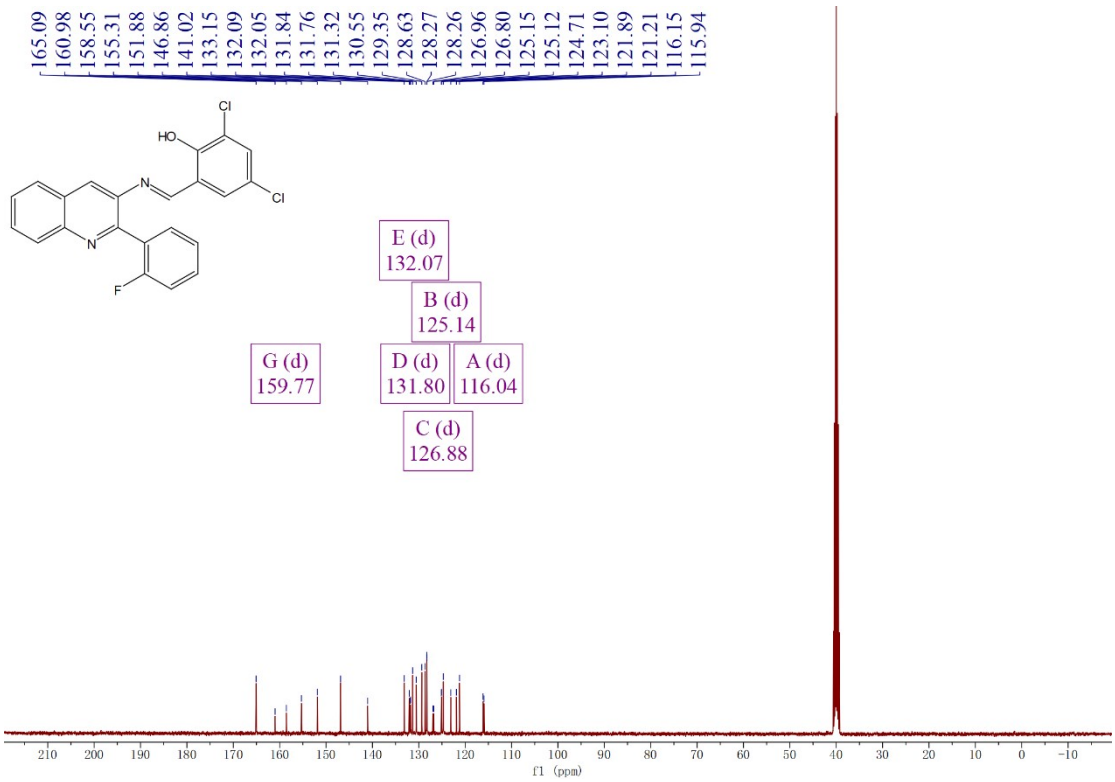

Figure S7. ^{13}C NMR (100MHZ, DMSO-d_6) spectrum of **L²**

Figure S8. ^{19}F NMR (376MHZ, DMSO-d_6) spectrum of **L²**

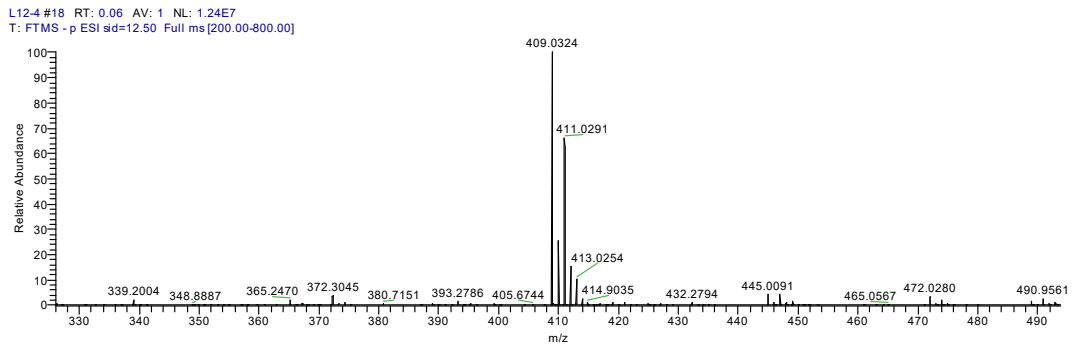

Figure S9. HRMS spectrum of **L²**

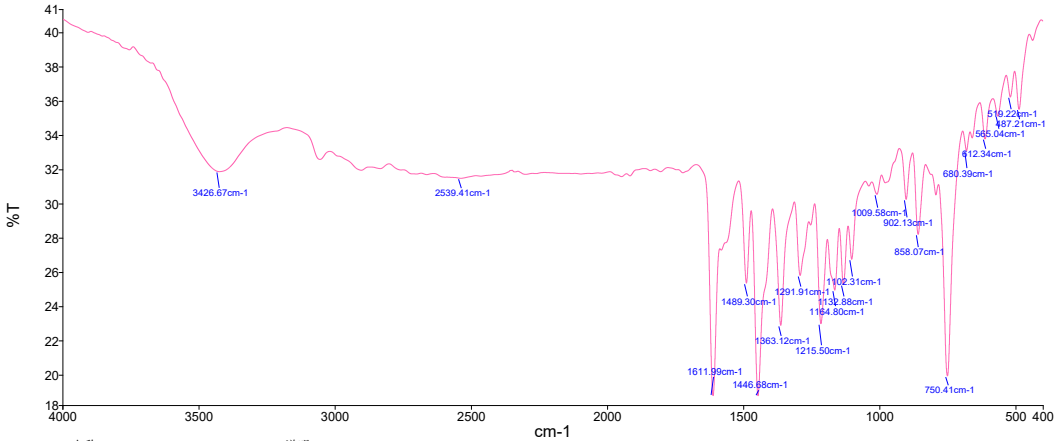

Figure S10. FT-IR spectrum of **L²**

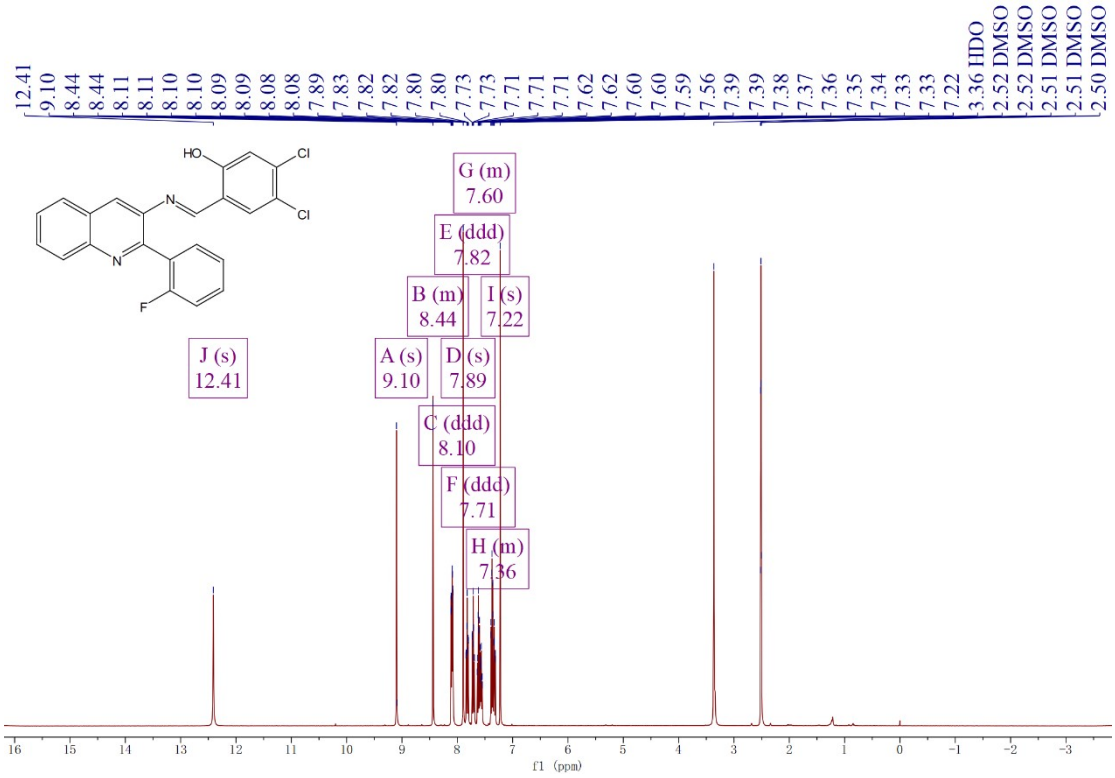

Figure S11. ^{1}H NMR (400MHZ, DMSO-d_6) spectrum of **L³**

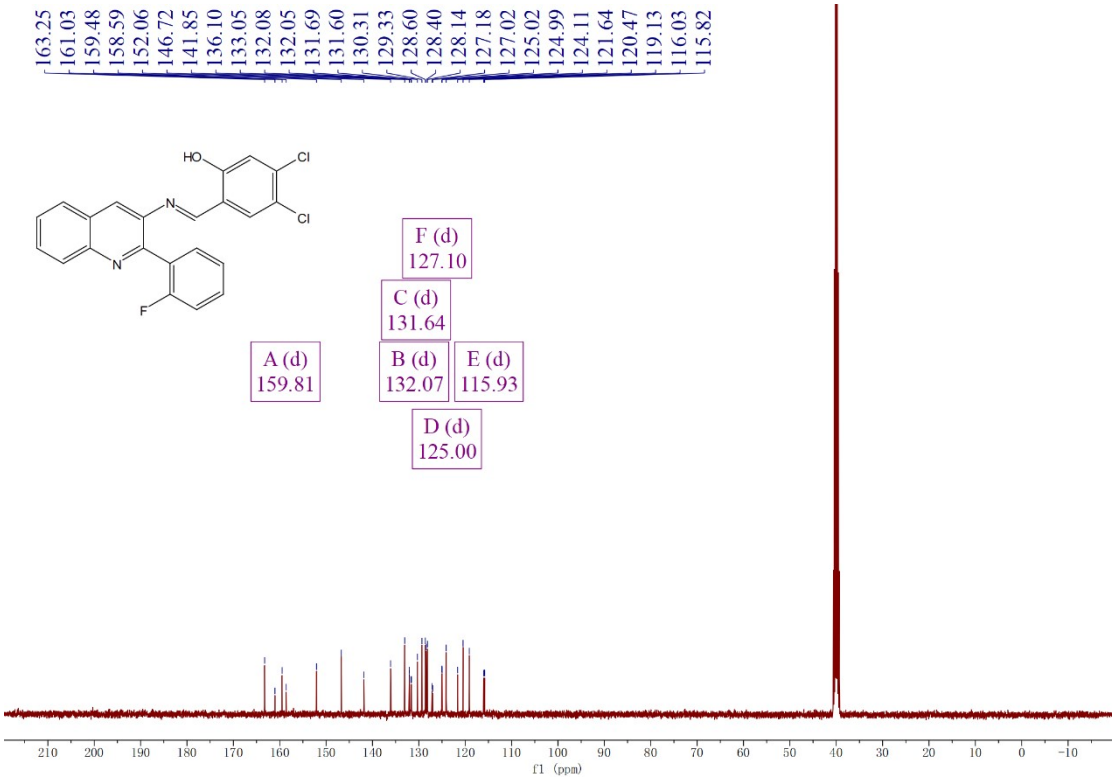

Figure S12. ^{13}C NMR (100MHZ, DMSO-d_6) spectrum of **L^3**

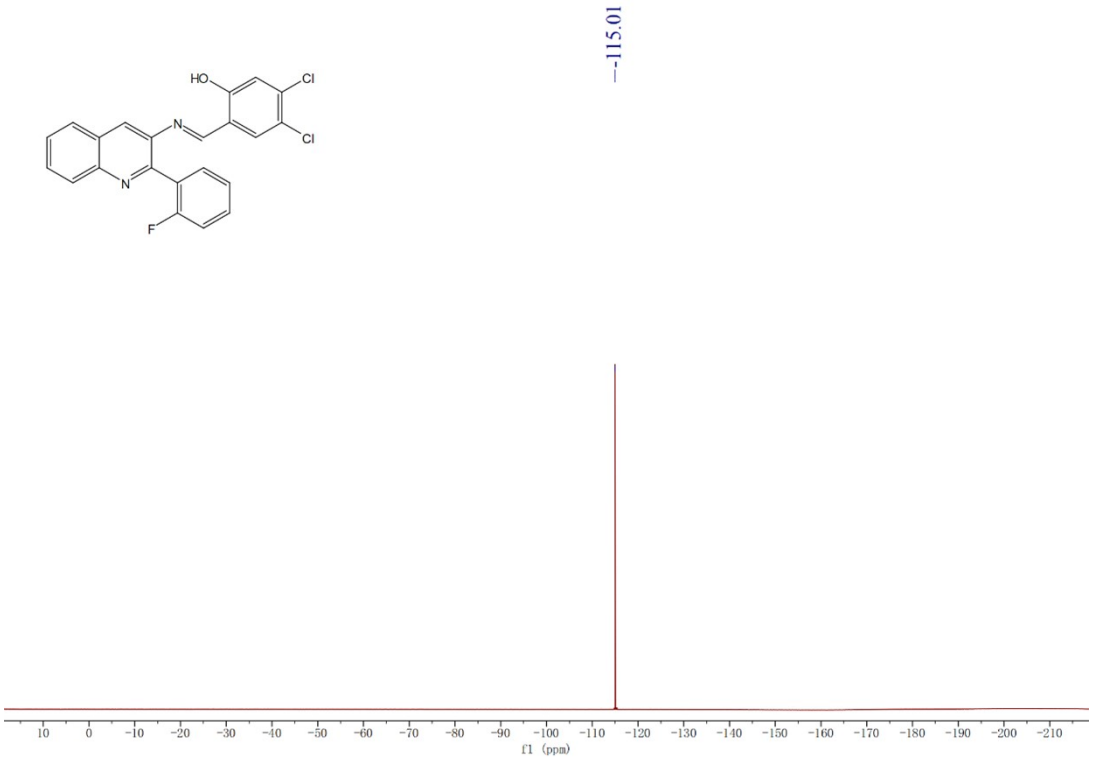

Figure S13. ^{19}F NMR (376MHZ, DMSO-d_6) spectrum of **L^3**

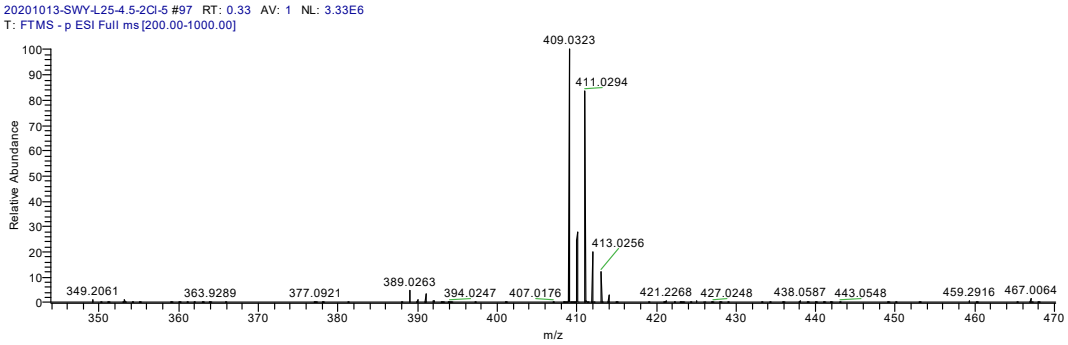

Figure S14. HRMS spectrum of **L^3**

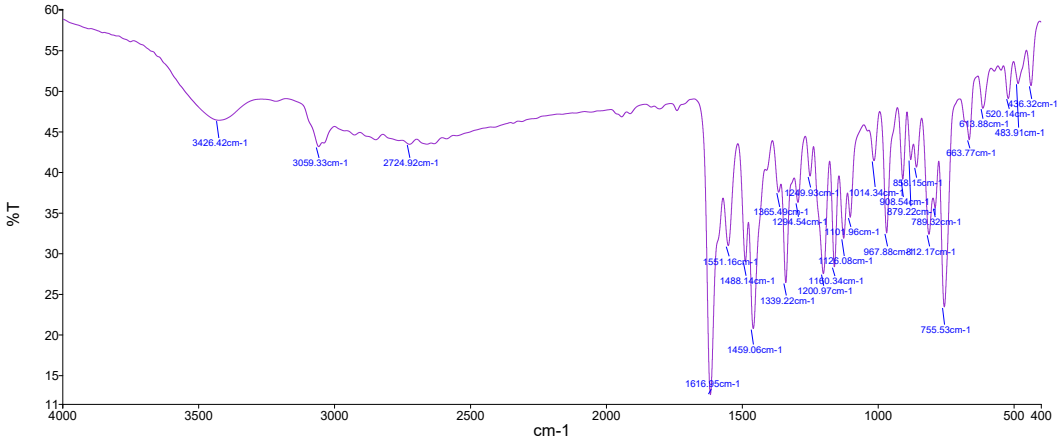

Figure S15. FT-IR spectrum of **L^3**

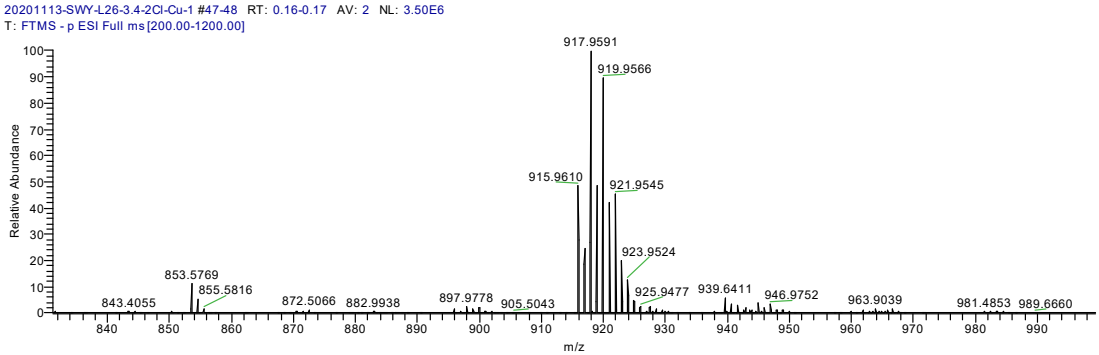

Figure S16. HRMS spectrum of **C1**

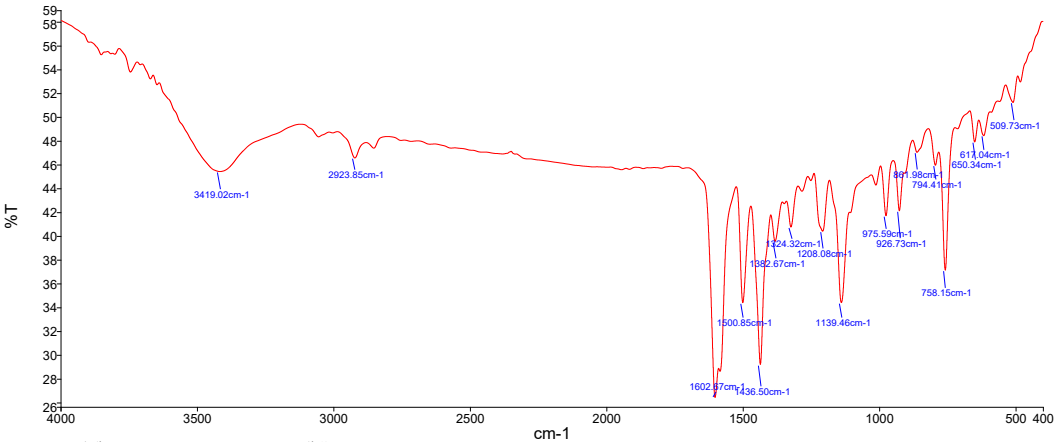

Figure S17. FT-IR spectrum of **C1**

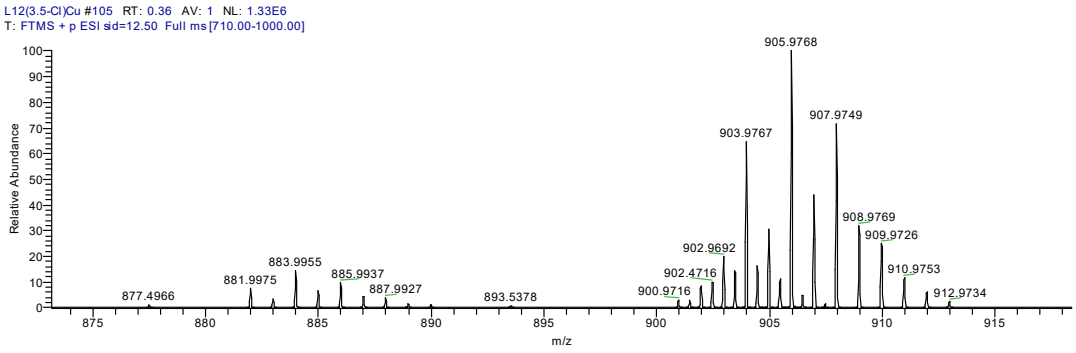

Figure S18. HRMS spectrum of **C2**

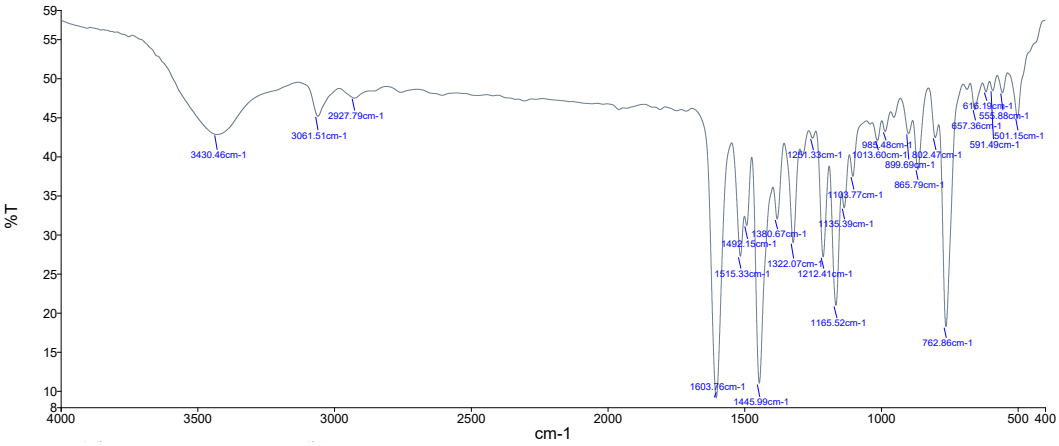

Figure S19. FT-IR spectrum of **C2**

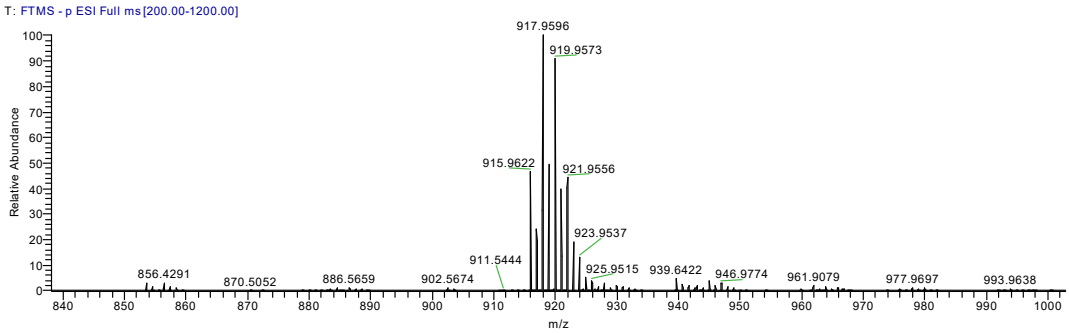

Figure S20. HRMS spectrum of **C3**

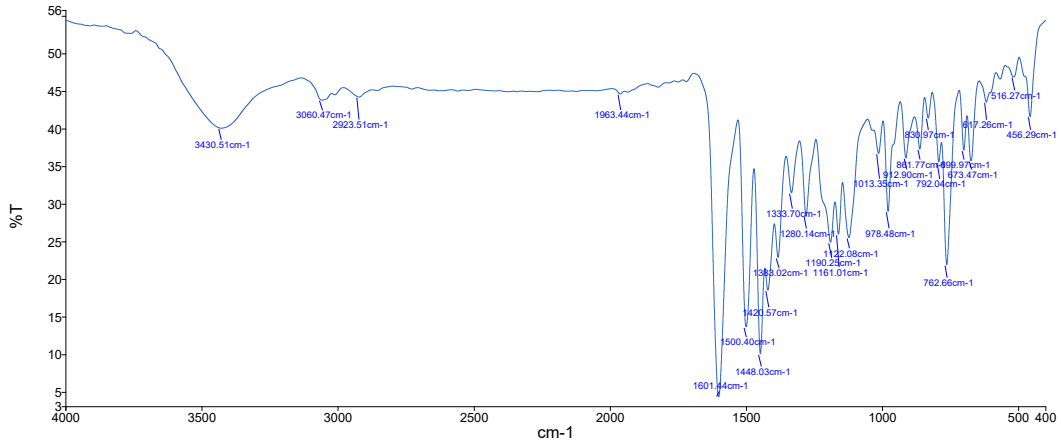

Figure S21. FT-IR spectrum of **C3**

UV-Vis spectra of C1–C3

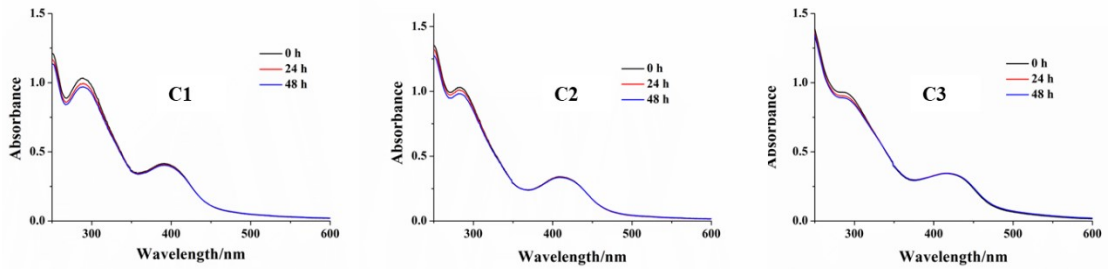

Figure S22. UV-Vis spectra of **C1**, **C2** and **C3** in PBS containing 1% DMF

HPLC trace of C1–C3

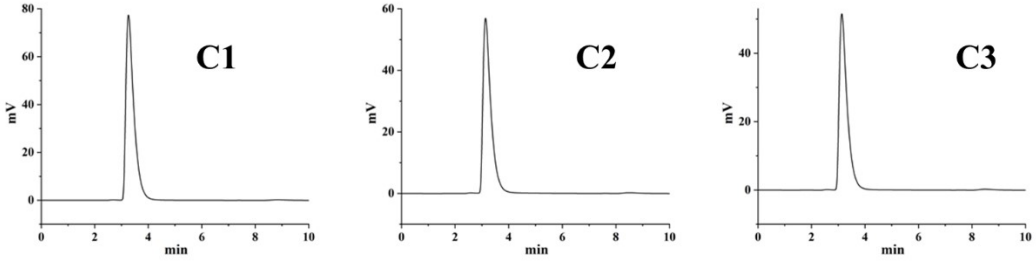

Figure S23. HPLC trace of **C1**, **C2** and **C3** in CH_3OH containing 1% DMF

H[1] NMR spectra of the reactions of C1–C3 with GSH

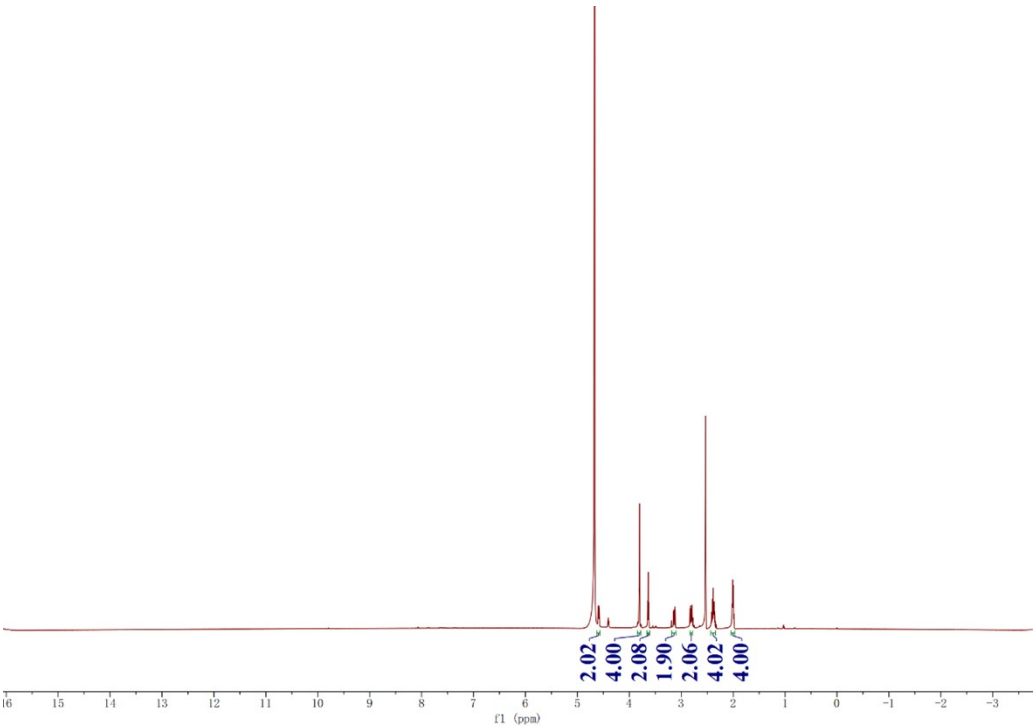

Figure S24. [1]H NMR (600MHz) spectrum of the reaction of **C1** with GSH (1:5 proportion of DMSO-*d6* and D_2O).

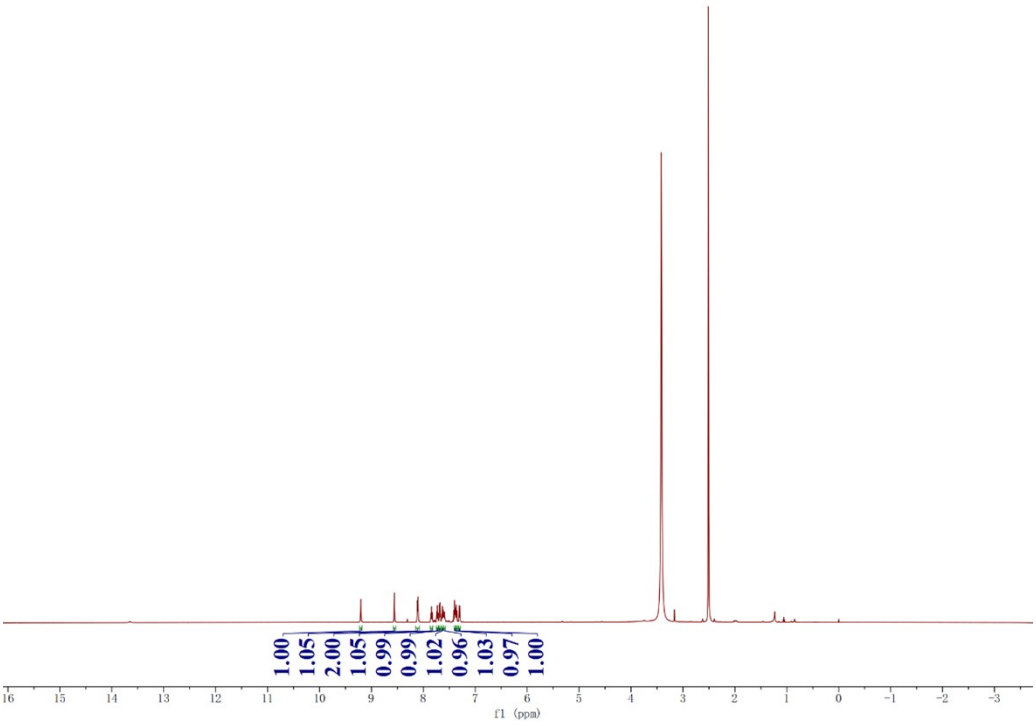

Figure S25. [1]H NMR (600MHz) spectrum of the reaction of **C1** with GSH (60:1 proportion of DMSO-*d6* and D_2O).

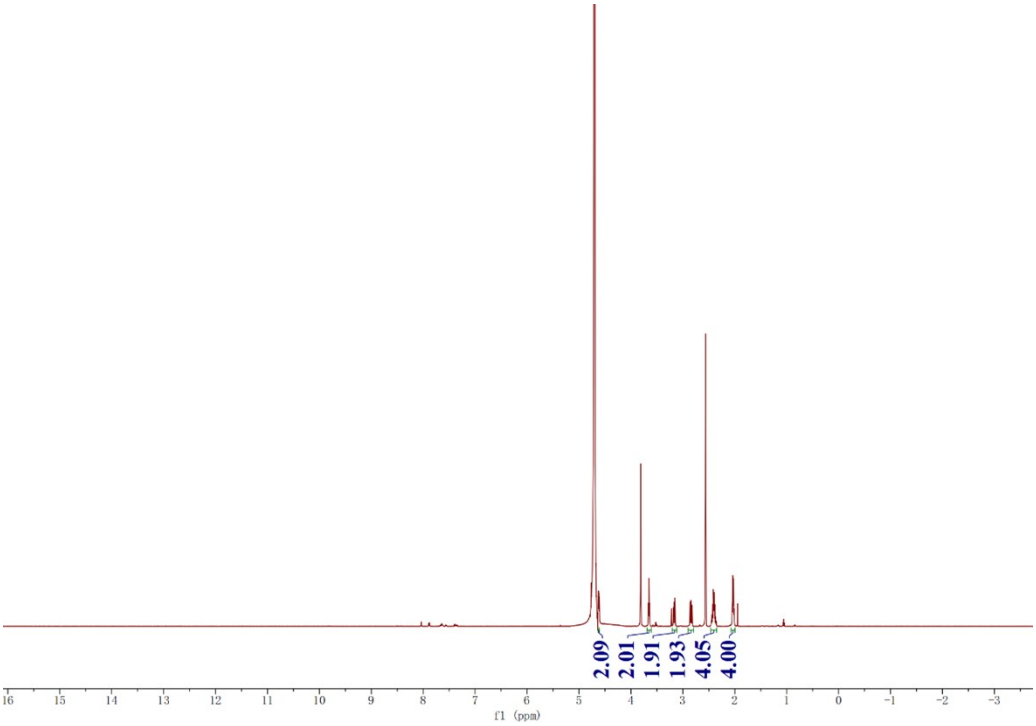

Figure S26. ^{1}H NMR (600MHz) spectrum of the reaction of **C2** with GSH (1:5 proportion of DMSO-*d6* and D_2O).

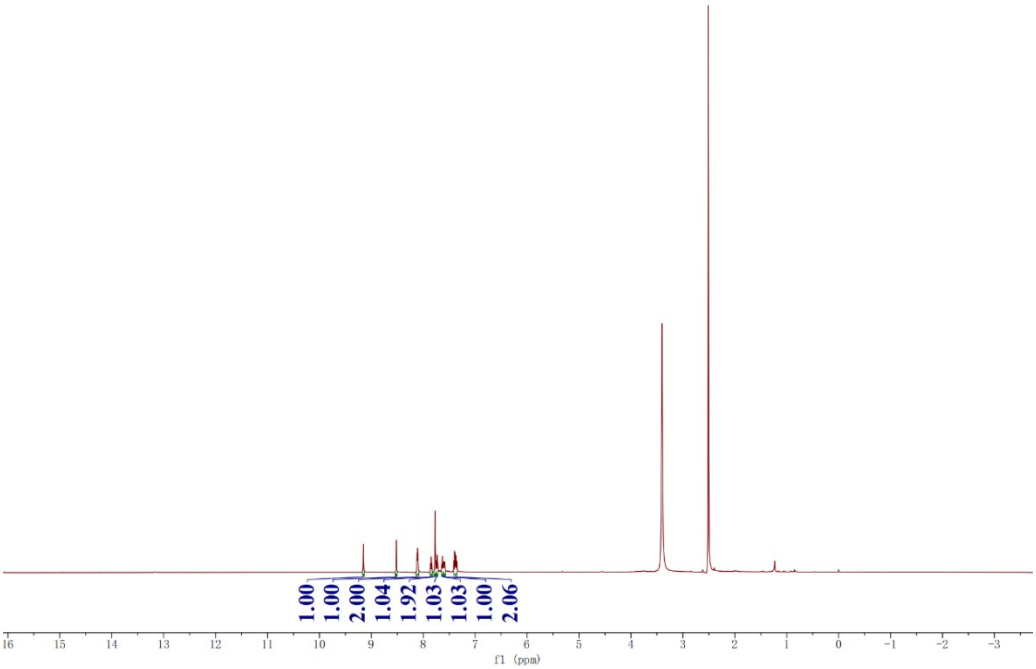

Figure S27. ^{1}H NMR (600MHz) spectrum of the reaction of **C2** with GSH (60:1 proportion of DMSO-*d6* and D_2O).

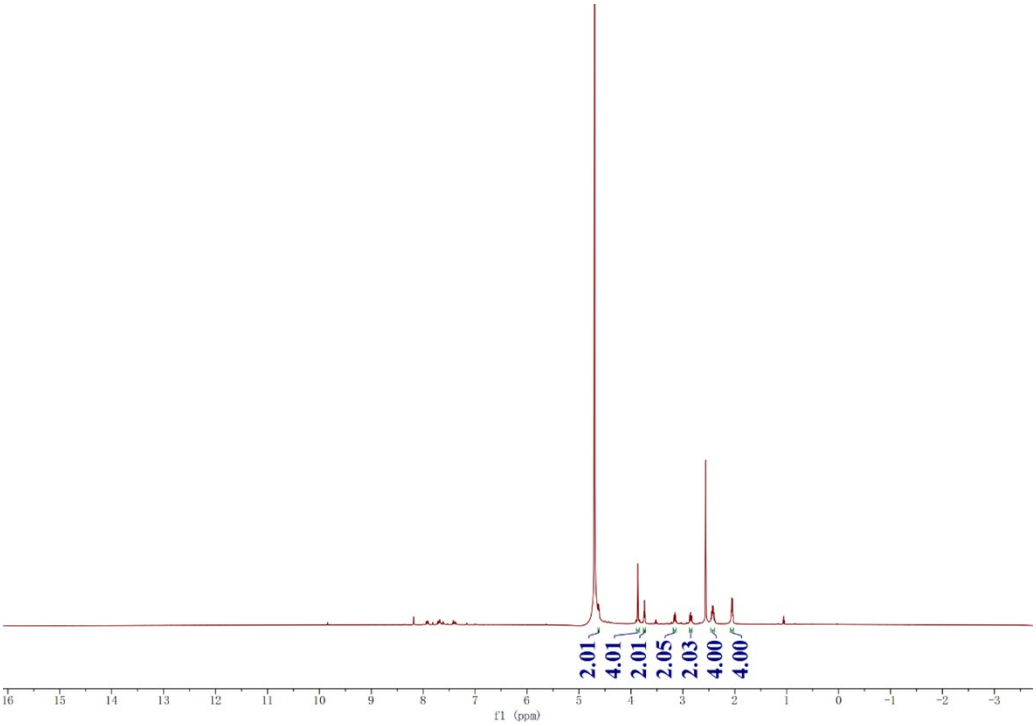

Figure S28. ^{1}H NMR (600MHz) spectrum of the reaction of **C3** with GSH (1:5 proportion of DMSO-*d6* and D_2O).

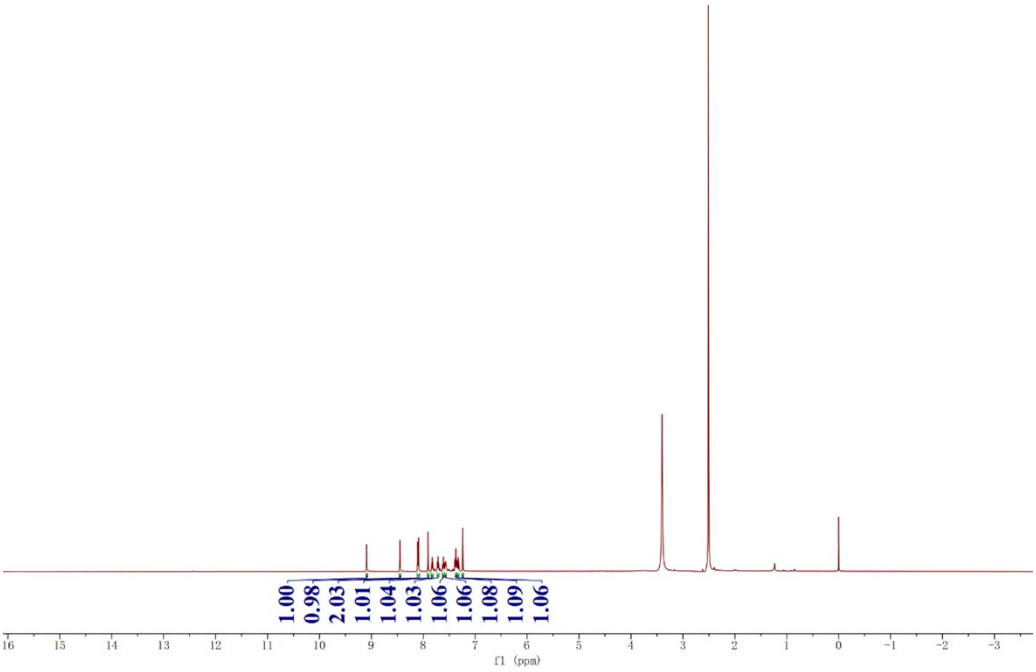

Figure S29. ^{1}H NMR (600MHz) spectrum of the reaction of **C3** with GSH (60:1 proportion of DMSO-*d6* and D_2O).

Crystal data of C1–C3

Table S1. A summary of crystallographic data of **C1**, **C2** and **C3**

	C1	**C2**	**C3**
Empirical formula	$C_{44}H_{24}Cl_4CuF_2N_4O_2$	$C_{44}H_{24}Cl_4CuF_2N_4O_2$	$C_{46}H_{32}Cl_4CuF_2N_4O_2$
Formula weight	884.01	884.01	948.09
Crystal system	Monoclinic	Monoclinic	Monoclinic
Space group	$P2_1/n$	$C2/c$	$C2/c$
a/Å	10.0633 (1)	19.6802 (6)	24.3709 (2)
b/Å	19.9246 (1)	9.9152 (2)	11.5828 (1)
c/Å	10.1296 (1)	20.2125 (6)	15.5789 (1)
α/°	90	90	90
β/°	110.210 (1)	94.951 (3)	102.622 (1)
γ/°	90	90	90
Volume/Å^3	1906.01 (3)	3929.39 (19)	4291.38 (6)
Z	2	4	4
ρcalcg/cm^3	1.540	1.494	1.467
μ/mm^{-1}	3.85	0.88	3.49
F(000)	894	1788	1932
CCDC	2115672	2115673	2115674

Table S2 Selected bond lengths[Å] and angles [°] of **C1**, **C2** and **C3**

	C1	**C2**	**C3**
Cu1—O1^i	1.9112 (11)	1.8933 (13)	1.9003 (11)
Cu1—O1	1.9113 (11)	1.8933 (13)	1.9002 (11)
Cu1—N1^i	1.9692 (13)	1.9941 (16)	1.9904 (13)
Cu1—N1	1.9692 (13)	1.9941 (16)	1.9903 (13)
O1^i—Cu1—O1	180.0	180.0	88.53 (7)
O1—Cu1—N1^i	89.19 (5)	91.15 (6)	149.69 (6)
O1—Cu1—N1	90.81 (5)	88.85 (6)	93.19 (5)
O1^i—Cu1—N1^i	90.81 (5)	88.85 (6)	93.18 (5)
O1^i—Cu1—N1	89.18 (5)	91.15 (6)	149.69 (6)
N1^i—Cu1—N1	180.0	180.0	100.18 (8)